

Automatic Fall Detection Based on Doppler Radar Motion Signature

Liang Liu, Mihail Popescu, Marjorie Skubic,
Marilyn Rantz
ECE Department of Missouri
Columbia, MO, USA
e-mail: llpfd@mail.missouri.edu,
{popescum, skubicm}@missouri.edu,

Tarik Yardibi, Paul Cuddihy
GE Global Research
Schenectady, NY, USA
e-mail: {yardibi,cuddihy}@ge.com

Abstract—Falling is a common health problem for elderly. It is reported that more than one third of adults 65 and older fall each year in the United States. To address the problem, we are currently developing a Doppler radar-based fall detection system. Doppler radar sensors provide an inexpensive way to recognize human activity. In this paper, we employed mel-frequency cepstral coefficients (MFCC) to represent the Doppler signatures of various human activities such as walking, bending down, falling, etc. Then we used two different classifiers, SVM and kNN, to automatically detect falls based on the extracted MFCC features. We obtained encouraging classification results on a pilot dataset that contained 109 falls and 341 non-fall human activities.

Keywords—fall detection; eldercare; MFCC features; radar classification; SVM; kNN

I. INTRODUCTION

Falls are the leading causes of accidental death in the US population over age 65 [1, 2]. In 2007, about three thirds of all people that died as a result of a fall were above age 65 [2]. The death rate caused by falls among elders is increasing quickly over the past decade [3]. Multiple studies showed that delay of the medical intervention after a fall is negatively correlated to its outcomes. If the nursing personnel is informed as soon as possible after a fall they can provide invaluable assistance that may significantly improve the intervention outcomes [4]. One of the possible solutions for reducing the intervention time is to automatically detect and then promptly report the fall to the related medical personnel.

In recently years, many fall detection methods have been described in the literature. There are two main types of fall monitoring devices: wearable and non-wearable. The simplest wearable device is a “Push-button”, which can be manually activated in case of a fall. Accelerometer-based wearable devices detect falls by measuring the applied acceleration along the vertical axis [5]. The wearable devices are inexpensive but they have two main drawbacks: they can’t be activated when a loss of conscience occurs after a fall and they may be not be worn at all times (for example, during night time) [6]. Among the non-wearable devices, we mention floor vibration sensors [7] and microphone arrays [8]. All these methods are currently under development and

show promising results. The main challenge of a fall detection system is to have as few false alarms as possible while detecting all the falls. In order to achieve this goal, we believe that it is necessary to develop multiple fall detection modalities together with multiple classification methods for each sensor and then combine them using a sensor fusion framework.

Various studies have shown that radar sensors can be employed for gait characterization. A Ku-band radar is used to estimate the gait velocity from the frequencies with the highest reflection levels. The stride rate can be estimated from the estimated gait velocities [9]. A continuous wave radar was used in [10] to estimate the stride rate by taking the Fourier transform at each Doppler frequency bin after computing the spectrogram. Different human body parts can generate different radar signatures [11]. Continuous wave radar can distinguish different persons and other moving objects [12]. A system using an acoustic Doppler radar and a microphone [13] showed that the footstep sounds correlated with the secondary peaks on the radar spectrogram. Another acoustic Doppler radar was used in [14] for human gait characterization studies with a training based classification method.

Many processing algorithms have been reported for radar data. Kim and Ling [15] extracted six features from a denoised radar spectrogram and used them to classify seven different human activities, such as running, walking, walking while holding a stick, crawling, boxing while moving forward, boxing while standing in place, and sitting still. The wavelet ridges and higher-order statistics were used in [16] characterize radar signals. A fuzzy support vector machine (SVM) was then applied to identify different emitter signals [16]. A successive normalization-based feature extraction algorithm on the instantaneous frequencies was obtained by using instantaneous autocorrelation in [17]. An intra-pulse feature extraction approach based on symbolic time series analysis (STSA) is proposed in [18]. The gait features are extracted to identify subjects in a realistic outdoor clutter background [19]. It has been shown that human operators that listen to the Doppler audio output from the surveillance radar are able to detect and identify certain targets [20]. It was concluded that the Doppler signature of targets can be manipulated by sound signal processing techniques.

Consequently, they [20] used mel-frequency cepstral coefficients (MFCC) features to represent the Doppler signatures and then they employed a Gaussian Mixture Model (GMM) to achieve about 88% target recognition rate.

In our paper, we propose a fall detection technique that involves two pulse-Doppler range control radars (RCR) developed by General Electric Co. RCR uses the Doppler principle to estimate the relative velocities of the targets within the detection range. RCR transmits the electromagnetic wave signal at a certain frequency and measures the various frequency shifts in the reflected wave. Different body parts generate distinct Doppler signatures for a certain moving person. Since a human fall comprises a series of human body parts movements, it is reasonable to try recognizing a fall based on its Doppler signature.

This paper is organized as follows. In section II, we describe the experimental setup and the available datasets. In section III, we present the algorithms employed in this work. In section IV, we present and analyze the experimental results. The conclusion is given in section V.

II. EXPERIMENT SETUP AND DATASET DESCRIPTION

The experimental setup is shown in the diagram from Fig. 1 and in the image shown in Fig. 2. RCR sensor A is placed at the end of a 24 foot long and 3 foot wide carpet. RCR sensor B is placed on the right side of the carpet (when the subject is facing RCR A) orthogonally to RCR A. During this experiment, test subjects are asked to perform different actions at the center of the carpet or walk toward RCR A.

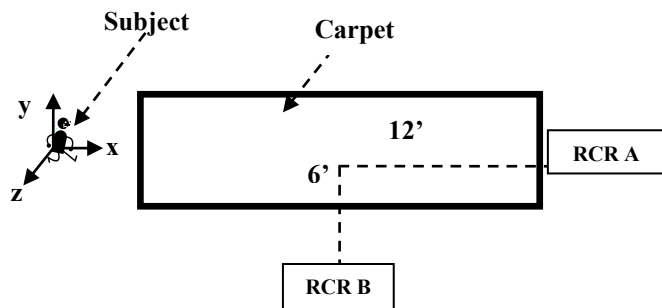


Figure 1. The diagram of the Doppler-based sensors fall detector setup.

In Fig. 2, the positions of the two sensors, RCR A and RCR B, are marked with red circles. Since a Doppler radar is sensitive mainly to movement along its central axis, more than one sensor might be necessary to ensure that falls in any direction can be detected. However, a sensor placed on the ceiling might be sufficient for a small room due to the fact that most falls have an important vertical motion component. There are advantages of this setup: the beam is not obstructed by objects in the room and there is no interference from the nearby hallway (since there is some amount of wall penetration of the radar beam). We mention that our initial setup (two radars placed on the floor) was motivated by our initial gait measurement experiments. We are currently collecting more data in order to investigate the fall detection performance of a single RCR sensor placed on the ceiling.



Figure 2. The Doppler-based sensors fall detector setup in lab.

The dataset used in this paper consists in 450 human activity radar signatures (see Table I): 109 falls and 341 possible false alarms (non falls). The falls were performed by two students and by a professional stunt actor. The stunt actor was trained by our nursing collaborators to fall like older adults. We replicated various types of falls such as forward fall, backward fall, left-side fall, right-side fall, etc. Relative to the sensor positions, we included different types of falls such as between the two sensors and towards or away from one of the sensors. Out of 109 falls, 98 fall signatures were recorded when both sensors were on floor and other 11 were recorded when RCR B was mounted on the ceiling and RCR A was placed on floor. The 341 “non fall” signatures were acquired from various activities performed by 8 human subjects (our entire team). Among the recorded human activities we mention bending over to pick up objects from the floor, kneeling, tying shoes, sitting on a chair, arm/leg swing, walking, etc.

The radar signals were recorded using a National Instruments data acquisition card NI 9201 with 8-channel analog inputs. The signal processing and classification of the recorded radar signal were performed using Matlab (<http://www.mathworks.com>).

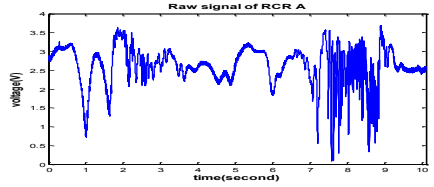
III. ALGORITHMS AND METHODS

The procedure employed to classify an activity as a “fall” or “not fall” based on its radar signature has the following steps:

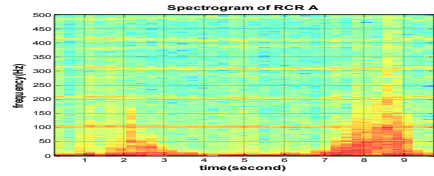
1. Compute the spectrogram ($STFT(f, t)$, see Fig. 3.b) of the entire radar signature (raw signal, see Fig. 3.a). The sampling frequency of the radar signal is 1000Hz.
2. Compute the energy burst curve (see Fig. 3.c). Through experimentation, we determined that the frequencies of interest for fall detection are in the [25-50] Hz range. Consequently the energy burst EB is computed as: $EB(t) = \sum_{25}^{50} STFT(f, t)$.
3. Find the location of the maximum, t_{max} , of the energy burst curve, $EB(t)$. We assumed that a fall is a catastrophic event that involves many body parts (hence many frequencies) that move with speeds

superior (hence produce high intensity Doppler signal) to most indoor activities. For example, in Fig. 3.a we can compare the signatures of two events: at $t \sim 2$ s the actor bent and clapped and at $t \sim 8$ s she fell. In Fig. 3.b, we clearly see that the fall spans a frequency range about 4 times larger than the bend-and-clap event, with higher energy levels at each frequency.

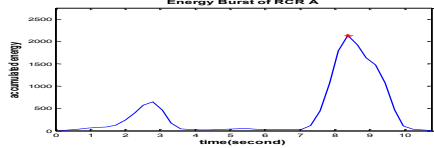
4. Compute the MFCC features in a 4-second window centered at the maximum energy location, t_{max} . We only use six MFCC coefficients in this paper (index 2 to 7). To make the system less dependent on the distance to the sound source, we did not use the first cepstral coefficient. The features were extracted using the Matlab function, *mfcc* [21]. The extracted features for a 4-second window are represented by a 6×174 matrix. We then arrange the feature matrix into a vector with $6 \times 174 = 1044$ elements that we further use in the classification algorithm.
5. We independently classify the feature vectors extracted from the signatures produced by the two radars, A and B. For each feature vector we used three classifiers: support vector machines (SVM) and k-nearest neighbor (kNN). Each classifier outputs a confidence, $conf \in [0,1]$, that the current activity signature represents a fall.



a.) Raw Doppler radar signal (a fall occurred at $t=8$)



b.) Spectrogram of the raw signal (spectrogram)



c.) The energy burst curve of the spectrogram. Peak value is marked by a red cross.

Figure 3. First three signal processing steps of a radar signature: a) raw signal, b) spectrogram and c) energy burst

6. Use a set of N thresholds, $\{\theta_i\}_{i=1,N}$ to compute the receiver operator characteristic (ROC) curve. By thresholding the confidence of each classifier with each threshold in the set we obtained N {detection rate, false alarm rate} pairs that are used to plot the ROC. The detection rate for each threshold was

computed as $(\# \text{ of falls detected})/109$ and the false alarm rate as $(\# \text{ false alarms})/341$.

IV. RESULTS

A. Sample outputs for the two RCR sensors

In Fig. 4, we show the raw Doppler signal, the spectrogram and the energy burst for a typical fall compared to the same measurements for a non-fall.

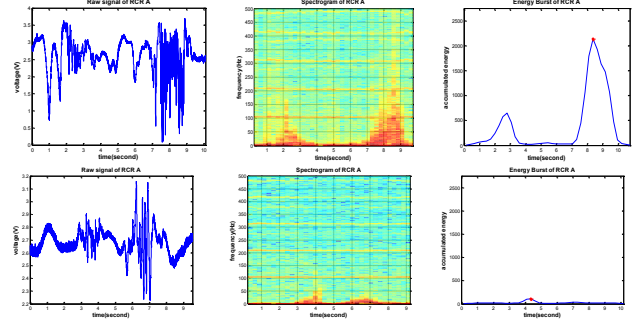


Figure 4. Doppler signal, spectrogram and energy burst captured by RCR sensor A, for a typical fall (upper row) and for a false alarm (lower row)

The false alarm (lower row in Fig. 4) was acquired when a student picked up a book from the floor. The first energy burst corresponds to bending down, while the second one represents coming back up. By comparing the pictures in the two rows of Fig. 4, we see that the energy burst of the fall is higher than that of false alarms. This is typically the case for older adults that do not perform very vigorous activities. Also, the spectral composition of a fall (upper spectrogram) seems to be different from the one of bending (lower spectrogram), with higher frequencies up to about 200 Hz for the fall case. This might be explained by the many body parts involved in a fall, which is rarely the case for regular indoor activities. These observations argue favorably for the possibility of using a classifier to detect the falls.

B. Performance of the SVM and kNN Classifiers

In Fig. 5 and 6 we show the ROCs obtained for the two classifiers (Fig. 5 – for RCA A, and Fig. 6 for RCA B) used in this paper, SVM and kNN.

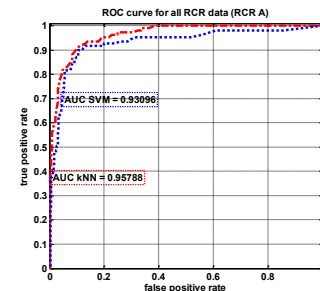


Figure 5. Performance results for kNN and SVM classifiers on RCR A data

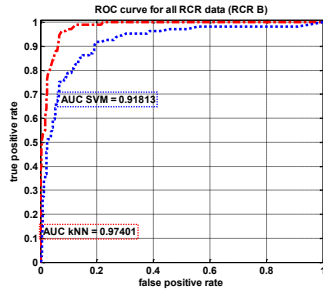


Figure 6. Performance results for kNN and SVM classifiers on RCA B data.

From the above results we see that kNN ($k=3$) produced the best results for both sensors, with an area under the curve (AUC) of about 0.96. SVM performance was close, with an AUC of about 0.92.

By analyzing the false alarms of both classification algorithms we found some examples of squatting and kneeling. A possible reason for this situation is that while the actor and the students were instructed how to walk and fall as an older adult, they were not told to bend and kneel in the same fashion. As a result, the speed of these actions was possibly close to that of a fall. We intend to address this problem by collecting data in a real living environment, the Tiger Place aging in place facility from Columbia, Missouri, where the stunt actor will perform only the falls but not the false alarms.

V. CONCLUSION

In this paper we present an automatic fall detection system based on two Doppler radar sensors. The radar sensor measures the relative speed of motion on a direction parallel to its emission axis. Since a human fall comprises a series of human body parts in motion, it is reasonable to try recognizing a fall based on its Doppler signature.

We used MFCC features to represent the activity signature. Then we used two well known classifiers, SVM and kNN, to classify the activities from a pilot dataset of about 450 samples in two classes: falls and non-falls. We consider the classification results obtained (AUC between 0.91 and 0.97) as encouraging.

In future work we plan to investigate the placement of a single sensor on the ceiling, employ classifier fusion to reduce the false alarm rate and collect datasets in a real living environment (Tiger Place).

ACKNOWLEDGEMENTS

This work has been supported in part by an AHRQ grant.

REFERENCES

- [1] Murhy SL, "Deaths: Final Data for 1998," *National Vital Statistics Reports*, vol. 48, no. 11. Hyattsville, Maryland: National Center for Health Statistics, 2000.
- [2] Centers for Disease Control and Prevention, National Center for Injury Prevention and Control. [Web-based Injury Statistics Query and Reporting System \(WISQARS\)](#) [online]. Accessed November 30, 2010
- [3] Stevens JA. Fatalities and injuries from falls among older adults – United States, 1993–2003 and 2001–2005. *MMWR* 2006a;55(45).

- [4] C. G. Moran, R.T. Wenn, M. Sikand, A.M. Taylor, Early mortality after hip fracture: is delay before surgery important", *J. of Bone and Joint Surgery*, pp. 483-9, 2005.
- [5] Giansanti D, Maccioni G and Macellari V, "The development and test of a device for the reconstruction of 3D position and orientation by means of a kinematic sensor assembly with rate gyroscopes and accelerometers," *IEEE Trans. Biomed. Eng.* **52** 1271–7, 2005
- [6] N. Noury, A. Fleury, P. Rumeau, et al., "Fall detection-principles and methods", Proc. of the 29th IEEE EMBS, Lyon, France, Aug. 23-26,
- [7] M. Alwan, P. J. Rajendran, S. Kell, D. Mack, S. Dalal, M. Wolfe, R. Felder, " A smart and passive floor-vibration based fall detector for elderly", 2nd IEEE Int. Conf. on Inf. & Comm. Tech.: from Theory to Applications - ICTTA'06, April 24 - 28, 2006, Damascus, Syria.
- [8] Y. Li, Z. Zeng, M. Popescu, D. Ho, "Acoustic Fall Detection Using a Circular Microphone Array", Proc. of 32nd Annual International Conference of the IEEE EMBS, Buenos Aires, Argentina, Aug. 31 - Sept. 4, 2010, pp. 2242-2245.
- [9] D. Tahmoush, J. Silvius, "Radar stride rate extraction," 13th International Machine Vision and Image Processing Conference, pp. 128-133, 2009
- [10] M. Otero, "Application of a continuous wave radar for human gait recognition," The MITRE Corporation, 2005.
- [11] J. L. Geisheimer, W. S. Marshall, E. Grenaker, "A continuous-wave (CW) radar for gait analysis," *Signals, Systems and Computers*, vol. 1, pp. 834-838, 2001.
- [12] C. Hornsteiner, J. Detlefsen, "Characterisation of human gait using a continuous-wave radar at 25 GHz," *Adv. Radio Sci.*, vol. 6, pp. 67-70, 2008.
- [13] Z. Zhang, P. O. Pouliquen, A. Waxman, A. G. Andreou, "Acoustic micro-Doppler radar for human gait imaging," *J Acoust Soc Am.*, vol. 121, no. 3, pp. 110-113, 2007.
- [14] K. Kalgaonkar, R. Bhiksha, "Acoustic Doppler Sonar for gait recognition," Mitsubishi Electric Research Laboratories, Inc., 2007.
- [15] Youngwook Kim; Hao Ling; , "Human Activity Classification Based on Micro-Doppler Signatures Using a Support Vector Machine," *Geoscience and Remote Sensing, IEEE Transactions on* , vol.47, no.5, pp.1328-1337, May 2009
- [16] Mingqiu, Ren; Jinyan, Cai; Yuanqing, Zhu; Jun, Han; , "Radar signal feature extraction based on wavelet ridge and high order spectra analysis," *Radar Conference, 2009 IET International* , vol., no., pp.1-5, 20-22 April 2009
- [17] Yunwei Pu; Weidong Jin; Ming Zhu; Laizhao Hu; , "Classification of Radar Emitter Signals Using Cascade Feature Extractions and Hierarchical Decision Technique," *Signal Processing, 2006 8th International Conference on* , vol.4, no., 16-20 Nov. 2006
- [18] Tao-Wei Chen; Wei-Dong Jin; , "Feature extraction of radar emitter signals based on symbolic time series analysis," *Wavelet Analysis and Pattern Recognition, 2007. ICWAPR '07. International Conference on* , vol.3, no., pp.1277-1282, 2-4 Nov. 2007
- [19] Tahmoush, D.; Silvius, J.; , "Stride rate in radar micro-doppler images," *Systems, Man and Cybernetics, 2009. SMC 2009. IEEE International Conference on* , vol., no., pp.4218-4223, 11-14 Oct. 2009
- [20] Hughes, E. J.; Lewis, M.; , "The Application of Speech Recognition Techniques to Radar Target Doppler Recognition: A Case Study," *High Resolution Imaging and Target Classification, 2006. The Institution of Engineering and Technology Seminar on* , vol., no., pp.145-152, 21-21 Nov. 2006
- [21] M. Slaney, "Auditory toolbox 2.0", <http://www.slaney.org/malcolm>.